Structure of the liquid semiconductor GeSe

1999 J. Phys.: Condens. Matter 11 7051

(http://iopscience.iop.org/0953-8984/11/37/302)

J. Phys.: Condens. Matter **11** (1999) 7051–7060. Printed in the UK PII: S0953-8984(99)04928-0

Structure of the liquid semiconductor GeSe

Ingrid Petri†, Philip S Salmon† and Henry E Fischer‡

† Department of Physics, University of Bath, Bath BA2 7AY, UK
‡ Institut Laue–Langevin, Avenue des Martyrs, F-38042 Grenoble Cédex, France

Received 2 June 1999

Abstract. The partial structure factors and pair distribution functions for liquid GeSe at 727(2) °C were measured by using the method of isotopic substitution in neutron diffraction. The results show that the liquid retains little memory of the high-temperature crystalline phase of GeSe. On melting, there is a reduction in the Ge–Se coordination number from 6 to 3.2(2) and both Ge–Ge and Se–Se homopolar bonds become features of the molten state with contact distances of 2.36(2) and 2.34(2) Å and coordination numbers of 0.8(1) and 0.22(3) respectively. The results are discussed by reference to the structures of molten CuSe and CuBr, which contain electronegative species of the same or similar size. The structure is also compared with that of the glass-forming network melt $GeSe_2$ and it is found that, unlike the latter, there is no strong indication of intermediate-range atomic ordering as manifest by a prominent first sharp diffraction peak in one of the measured partial structure factors.

1. Introduction

The object of this paper is to present the full set of partial structure factors and pair distribution functions for the liquid semiconductor GeSe. Motivation for the study of this system stems, in part, from the observation that the nature of the bonding in liquid Ge_xSe_{1-x} ($0 \leqslant x \leqslant 1$) compounds changes from metallic to covalent as x is decreased from unity (see e.g. Salmon and Liu 1994). Also, it becomes possible to form bulk-quenched glasses over a wide range of composition, namely $0.43 \geqslant x \geqslant 0$ (Tronc *et al* 1973, Azoulay *et al* 1975). In order to understand this evolution in the bonding, the appearance of a glass forming region, and to test, for example, molecular dynamics results (Vashishta *et al* 1989a, b, Cobb and Drabold 1997, Massobrio *et al* 1998, 1999, Haye *et al* 1998), maximum information on the pair distribution functions is required. Furthermore, this knowledge is necessary to help explain the change in the local order of GeSe on melting wherein the coordination number of Ge changes from six to about four (Salmon and Liu 1994, Petri *et al* 1999). Ge and Se have close atomic numbers and sizes and for natural isotopic abundances their coherent neutron scattering lengths are similar. It is not therefore possible to resolve the local coordination environments of Ge and Se by using conventional neutron or x-ray diffraction methods to measure total structure factors or by using the x-ray absorption fine structure technique.

Molten GeSe is a semiconductor with an electrical conductivity $\sigma \approx 40\ \Omega^{-1}\ \mathrm{cm}^{-1}$ just above its melting point and positive temperature coefficient $\mathrm{d}\sigma/\mathrm{d}T$ (Ruska and Thurn 1976, Okada *et al* 1996). Thermopower measurements are consistent with p-type conductivity (Okada *et al* 1996) while the sign of the Hall coefficient is reported to change from positive to negative on melting (Glazov *et al* 1987). An interpretation of the Hall coefficient in disordered materials is however problematic (Cusack 1987).

0953-8984/99/377051+10$30.00

In the first part of this paper the results for the structure of molten GeSe are presented and the local coordination environments of the atomic species are compared with those in both the low and high temperature forms of the GeSe crystal structure. Next, the structure is discussed by reference to that of the molten AX materials CuSe (Barnes and Enderby 1988) and CuBr (Allen and Howe 1992, Saito *et al* 1997, Pusztai and McGreevy 1998) where A and X denote the electropositive and electronegative species respectively. These three AX systems have the same or similarly sized anions and structural information on CuSe and CuBr is also available at the partial pair-distribution function level. Finally, the structure of liquid GeSe is compared with that of the glass-forming network melt $GeSe_2$ (Penfold and Salmon 1990, 1991, 1992).

2. Theory

Consider three samples ${}^{N}\mathrm{Ge}{}^{N}\mathrm{Se}$, ${}^{70}\mathrm{Ge}{}^{N}\mathrm{Se}$ and ${}^{73}\mathrm{Ge}{}^{76}\mathrm{Se}$, where N denotes the natural isotopic abundance, that are identical in every respect except for their isotopic compositions. In a neutron diffraction experiment on these samples, the coherent scattered intensity can be represented by the total structure factors ${}^{N}_{N}F(Q)$, ${}^{70}_{N}F(Q)$ and ${}^{73}_{76}F(Q)$ respectively where in matrix notation

$$\begin{pmatrix} {}^{N}_{N}F(Q) \\ {}^{70}_{N}F(Q) \\ {}^{73}_{76}F(Q) \end{pmatrix} = \begin{pmatrix} 0.1675(8) & 0.3262(9) & 0.1588(4) \\ 0.250(5) & 0.399(4) & 0.1588(4) \\ 0.065(1) & 0.311(4) & 0.372(6) \end{pmatrix} \begin{pmatrix} S_{GeGe}(Q)-1 \\ S_{GeSe}(Q)-1 \\ S_{SeSe}(Q)-1 \end{pmatrix}. \tag{1}$$

In this equation the weighting coefficients are quoted in units of barns and were calculated using bound coherent scattering lengths of $b({}^{N}\mathrm{Ge}) = 8.185(20)$ fm, $b({}^{70}\mathrm{Ge}) = 10.0(1)$ fm, $b({}^{73}\mathrm{Ge}) = 5.09(4)$ fm, $b({}^{N}\mathrm{Se}) = 7.970(9)$ fm and $b({}^{76}\mathrm{Se}) = 12.2(1)$ fm. The latter correspond to the isotopic enrichments used in the neutron diffraction experiment (see section 3) while the scattering lengths and cross sections were taken from Sears (1992). The so-called Faber–Ziman partial structure factors, $S_{\alpha\beta}(Q)$, are obtained from inversion of equation (1) to give

$$\begin{pmatrix} S_{GeGe}(Q)-1 \\ S_{GeSe}(Q)-1 \\ S_{SeSe}(Q)-1 \end{pmatrix} = \begin{pmatrix} -45.3 & 33.0 & 5.3 \\ 37.9 & -23.8 & -6.0 \\ -23.7 & 14.1 & 6.8 \end{pmatrix} \begin{pmatrix} {}^{N}_{N}F(Q) \\ {}^{70}_{N}F(Q) \\ {}^{73}_{76}F(Q) \end{pmatrix}. \tag{2}$$

A measure of the conditioning of this matrix is provided by its normalized determinant $|A_n| = -0.02$ (Edwards *et al* 1975). The partial structure factors are related to the partial pair distribution functions, $g_{\alpha\beta}(r)$, through

$$g_{\alpha\beta}(r) = 1 + \frac{1}{2\pi^2 r n_0}\int_0^\infty Q[S_{\alpha\beta}(Q)-1]\sin(Qr)\,\mathrm{d}Q \tag{3}$$

where Q is the magnitude of the scattering vector and n_0 is the atomic number density. The mean number of particles of type β contained in a volume defined by two concentric spheres of radii r_i and r_j, centred on a particle of type α, is given by

$$\bar{n}^{\beta}_{\alpha} = 4\pi n_0 c_\beta \int_{r_i}^{r_j} r^2 g_{\alpha\beta}(r)\,\mathrm{d}r. \tag{4}$$

3. Experimental procedure

The isotopes, supplied by Europa Scientific UK, were freshly separated and immediately sealed under vacuum in glass ampoules for transportation to our laboratory. The GeSe samples were prepared by loading into silica ampoules ${}^{N}\mathrm{Ge}$ (99.9999%, Aldrich), ${}^{70}\mathrm{Ge}$ (99.8% ${}^{70}\mathrm{Ge}$, 0.2% ${}^{72}\mathrm{Ge}$) or ${}^{73}\mathrm{Ge}$ (98% ${}^{73}\mathrm{Ge}$, 0.3% ${}^{70}\mathrm{Ge}$, 0.8% ${}^{72}\mathrm{Ge}$, 0.8% ${}^{74}\mathrm{Ge}$, 0.1% ${}^{76}\mathrm{Ge}$) together with ${}^{N}\mathrm{Se}$

(99.999%, Johnson Matthey) or ^{76}Se (99.75% ^{76}Se, 0.2% ^{74}Se, 0.05% ^{77}Se) in a high purity argon-filled glove box ($\approx$1 ppm oxygen, $<$10 ppm water). The ampoules had been cleaned using chromic acid prior to etching with a 40% solution of hydrofluoric acid. The sample-filled ampoules were then evacuated to a pressure of $\approx 10^{-5}$ Torr, purged three times with helium gas, and after $\approx$48 h they were sealed. Each ampoule was itself subsequently sealed under vacuum in a larger silica container to ensure that if the inner silica cell cracked during the cooling phase of the subsequent heat treatment the sample would remain pure. The double-walled ampoules were loaded into a rocking furnace, slowly heated to 800 °C where they were left for $\approx$43 h, and cooled at 1 °C min^{-1} to room temperature. The crystalline GeSe samples were then transferred to matched cylindrical silica tubes of 5 mm internal diameter and 1 mm wall thickness and sealed under vacuum ready for the neutron diffraction experiments. The latter were made using the D4B instrument at the Institut Laue–Langevin, Grenoble with an incident wavelength of 0.7051 Å.

The complete diffraction experiment comprised the measurement of the scattering intensities at 727(2) °C for the samples contained in silica cells placed within a cylindrical vanadium heater; an empty silica cell in the heater and the empty heater. Each diffraction pattern was built up by making repeated scans of the detectors over the available range of scattering angles. No deviation was observed between scans, apart from the expected statistical variations (Jal *et al* 1990). The diffraction pattern for a cadmium bar of diameter 5 mm placed in the heater was also measured at room temperature for making the low-angle background correction (Bertagnolli *et al* 1976). The diffraction pattern for a vanadium rod of diameter 6 mm was used for the data normalization. The data analysis procedure followed that described elsewhere (Salmon 1988) and the liquid temperature was the same as that chosen previously (Salmon and Liu 1994). At this temperature the number density is 0.0387(2) Å^{-3} (Ruska and Thurn 1976) and the liquid forms a single homogeneous phase: the measured diffraction patterns show no small angle scattering and electrical conductivity (Okada *et al* 1996) and sound velocity (Tsuchiya 1990) experiments show no evidence of phase separation.

4. Results

The measured total structure factors are shown in figure 1 together with the Fourier back-transforms of the corresponding real-space functions obtained after setting the unphysical low-r oscillations for each function to their calculated limiting value. The good overall agreement between the data and back-transform at all Q-values indicates that the data correction procedure has been properly undertaken (Salmon and Benmore 1992). In figure 2 the $S_{\alpha\beta}(Q)$, obtained by direct inversion of these total structure factors using equation (2), are shown by the error bars and cubic spline fits to these $S_{\alpha\beta}(Q)$ are shown by the solid curves. The corresponding $g_{\alpha\beta}(r)$ are given in figure 3 as broken and full curves respectively. The measured partial structure factors fully satisfy the sum rules and inequality relations given by Edwards *et al* (1975). They give $g_{\alpha\beta}(r)$ that oscillate about the correct low-r limit and there is no trace of a peak at the Si–O bond length of 1.6 Å, which would arise from an incorrect silica container correction (Barnes *et al* 1997). A summary of the mean atomic distances and coordination numbers obtained from the $g_{\alpha\beta}(r)$ is given in table 1.

Figure 4 shows the total structure factors decomposed into the Bhatia–Thornton (1970) partial structure factors $S_{ij}^{BT}(Q)$. In this formalism $S_{NN}^{BT}(Q)$, $S_{NC}^{BT}(Q)$ and $S_{CC}^{BT}(Q)$ denote the number–number, number–concentration and concentration–concentration partial structure factors respectively. The Fourier transform of $S_{NN}^{BT}(Q)$ is denoted by $g_{NN}^{BT}(r)$ and describes the sites of the scattering nuclei but does not distinguish between the different chemical species occupying those sites. It is therefore measured directly if the bound coherent scattering lengths

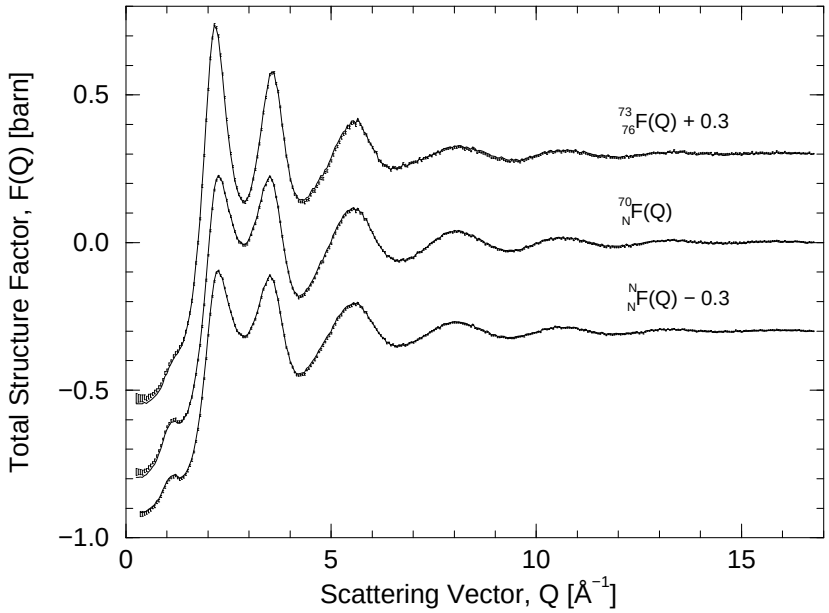

Figure 1. The measured total structure factors ${}^{N}_{N}F(Q)$, ${}^{70}_{N}F(Q)$ and ${}^{73}_{76}F(Q)$ for molten GeSe at 727(2) °C. The bars represent the statistical errors on the data points and the solid curves are the Fourier back-transforms of the corresponding real-space functions obtained after setting the unphysical low-r oscillations for each function to their calculated limiting value.

Table 1. Interatomic distances and coordination numbers in liquid GeSe at 727(2) °C.

$g_{\alpha\beta}(r)$	First peak position (Å)	$\bar{n}^{\beta}_{\alpha}$	Integration range (Å)	Second peak position (Å)	$\bar{n}^{\beta}_{\alpha}$	Integration range (Å)
$g_{GeGe}(r)$	2.36(2)	0.8(1)	1.96–2.91	3.81(2)	7.4(3)	2.91–4.85
$g_{GeSe}(r)$	2.54(2)	3.2(2)	2.15–3.10	≈ 3.5[a]	2.1(2)[a]	3.10–3.93[a]
$g_{SeSe}(r)$	2.34(2)	0.22(3)	1.90–2.64	3.76(2)	8.6(3)	3.01–4.85

[a] Corresponds to the first shoulder in $g_{GeSe}(r)$.

of the nuclei are equal. This is almost the case for the ^{N}Ge^{N}Se measurement and hence $S^{BT}_{NN}(Q)$ is known to good precision.

5. Discussion

5.1. Comparison with the high- and low-temperature crystal structures of GeSe

The low-temperature form of crystalline GeSe, LT-GeSe, has a distorted NaCl-type structure in which each chemical species makes six bonds, three weaker than the other three, to unlike chemical species to form a double-layer structure (Okazaki 1958, Kannewurf *et al* 1960, Dutta and Jeffrey 1965, Hulliger 1976). At 651(5) °C it undergoes a structural phase transition to the high-temperature phase, HT-GeSe, which has a normal NaCl-type structure (Wiedemeier and Siemers 1975, Petri *et al* 1999) before melting at 675(2) °C (Ipser *et al* 1982). The fractional volume change $(V' - V)/V$ is 0.5% for the solid–solid phase transition and 9% for the melting transition (Ruska and Thurn 1976, Wiedemeier and Siemers 1975), where V' and V denote the volumes for temperatures just above and below the transition of interest.

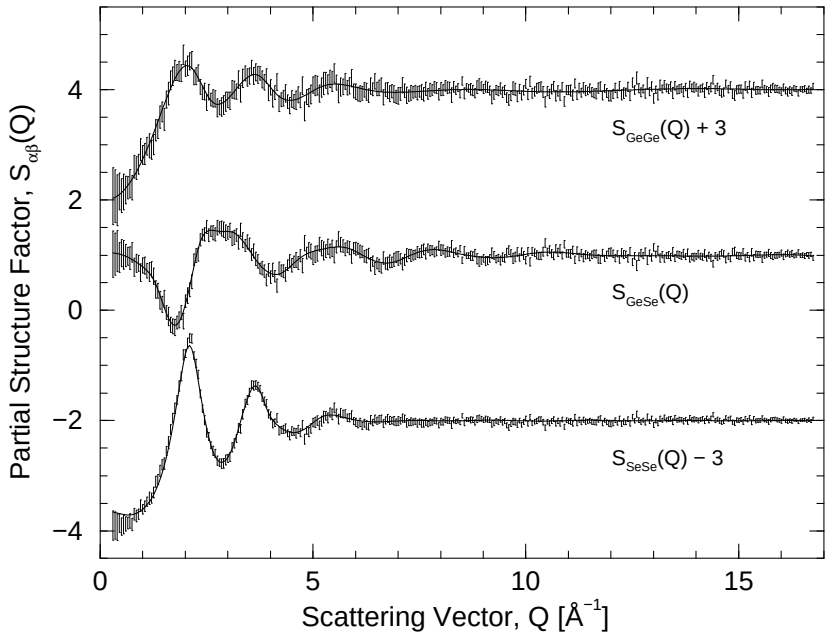

Figure 2. The experimental partial structure factors $S_{GeGe}(Q)$, $S_{GeSe}(Q)$ and $S_{SeSe}(Q)$ for molten GeSe at 727(2) °C. The bars represent the statistical errors on the data points and the solid curves are the smoothed $S_{\alpha\beta}(Q)$ obtained by using a cubic spline fit to the data points.

In the liquid $g_{GeSe}(r)$ has a first peak at 2.54(2) Å and a shoulder at ≈3.5 Å. The first peak gives a Ge–Se coordination number of 3.2(2) which increases to 5.3(3) if the shoulder extending from 3.10 Å to 3.93 Å is included in the integration range. HT-GeSe comprises Ge centred octahedra with six Ge–Se bonds at 2.87 Å (Wiedemeier and Siemers 1975) while in LT-GeSe each Ge has one Se at 2.56 Å and two Se at 2.59 Å followed by two Se at 3.32 Å and one Se at 3.37 Å (Dutta and Jeffrey 1965). On melting, the octahedra of HT-GeSe are therefore disrupted and the first-nearest-neighbour Ge–Se correlations in the melt resemble those in LT-GeSe.

Homopolar Ge–Ge and Se–Se bonds occur in the liquid as represented by the low-r peaks in $g_{GeGe}(r)$ and $g_{SeSe}(r)$. These peaks are considered to be real since their removal, by setting them equal to the limiting value of $g_{\alpha\beta}(r) = 0$, leads to a detrimental agreement between the corresponding $S_{\alpha\beta}(Q)$ and the Fourier back-transform of the resultant $g_{\alpha\beta}(r)$. Furthermore, the peak positions represent reasonable bonding distances. For example, the Ge–Ge bonds appear in the liquid at a distance 2.36(2) Å that is intermediate between 2.33(3) Å estimated for molten $GeSe_2$ (Penfold and Salmon 1991) and 2.45–2.47 Å observed in crystalline or amorphous Ge (Etherington *et al* 1982, Dalba *et al* 1995). Also, the Se–Se bond length of 2.34(2) Å is comparable to that found in liquid and amorphous Se (see e.g. Hohl and Jones 1991). Moreover, the Ge–Ge homopolar bonding coordination number of 0.8(1) and the Ge–Se first-nearest-neighbour coordination number of 3.2(2) are fully consistent with the results obtained from a previously reported first-order difference experiment on liquid GeSe (Petri *et al* 1999). This is significant since several types of systematic error are reduced or essentially eliminated in first-order difference experiments (see e.g. Salmon *et al* 1998).

In HT-GeSe, Ge has 12 nearest-neighbour Ge at 4.05 Å (Wiedemeier and Siemers 1975) while in LT-GeSe these 12 nearest-neighbour Ge are distributed between 3.40 and 4.73 Å (Dutta

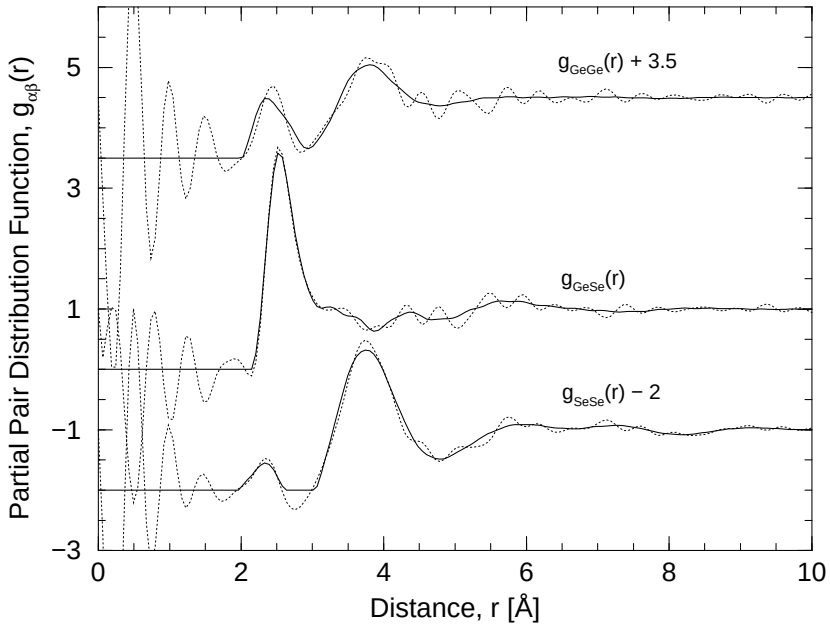

Figure 3. The $g_{\alpha\beta}(r)$ for molten GeSe at 727(2) °C obtained from the $S_{\alpha\beta}(Q)$ shown in figure 2. The solid curves are the Fourier transforms of the smoothed $S_{\alpha\beta}(Q)$ given by the solid curves in figure 2 and the broken curves are the Fourier transforms of the unsmoothed $S_{\alpha\beta}(Q)$ given by the error bars in figure 2.

and Jeffrey 1965). On melting, the Ge–Ge coordination environment in HT-GeSe is therefore disrupted to give an average of 0.8(1) Ge–Ge homopolar contacts together with 7.4(3) Ge–Ge next-nearest neighbours distributed between 2.91 and 4.85 Å. Furthermore, in HT-GeSe, Se has 12 nearest-neighbour Se at 4.05 Å (Wiedemeier and Siemers 1975) while in LT-GeSe there are ten nearest-neighbour Se distributed between 3.68 and 4.40 Å and two further Se at 5.74 Å (Dutta and Jeffrey 1965). Again, the Se–Se coordination environment in HT-GeSe is disrupted on melting to give an average of 0.22(3) Se–Se homopolar contacts together with 8.6(3) Se–Se next-nearest neighbours distributed between 3.01 and 4.85 Å.

Overall, the liquid retains little memory of the HT-GeSe solid phase. Furthermore, although both the first-nearest-neighbour Ge–Se distance and coordination number in the melt are comparable to those in LT-GeSe, Ge is not 3+3 coordinated to Se but is fourfold coordinated to 3.2(2) Se and 0.8(1) Ge. The 9% volume change on melting is therefore accompanied by a collapse of the local cubic close packing associated with HT-GeSe.

5.2. Comparison with the structure of molten CuSe and CuBr

It is instructive to compare the structure of liquid GeSe with that of the AX liquids CuSe (Barnes and Enderby 1988) and CuBr (Allen and Howe 1992, Saito *et al* 1997, Pusztai and McGreevy 1998) for which partial structure factors are also available. All three systems contain the same or similarly sized electronegative species (X = Se or Br) but have somewhat different physical characteristics. For example, CuSe melts at ≈525 °C from a structure wherein two thirds of the Se form pairs, with a characteristic bond length of 2.28 Å (Berry 1954), to give a molten semiconductor with a high electrical conductivity of 1240(20) Ω^{-1} cm^{-1} at 540 °C (Barnes and Enderby 1988). By comparison, CuBr melts at 488 °C from a high-temperature superionic

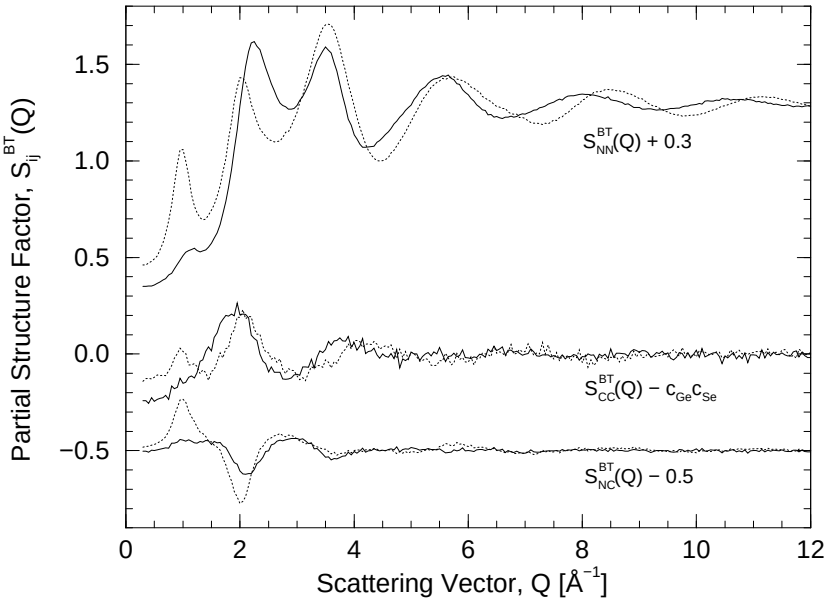

Figure 4. The experimental Bhatia–Thornton partial structure factors $S_{NN}^{BT}(Q)$, $S_{NC}^{BT}(Q)$ and $S_{CC}^{BT}(Q)$ for molten GeSe at 727(2) °C (solid curves) and molten $GeSe_2$ at 784(3) °C (broken curves). The atomic fractions of Ge and Se are denoted by c_{Ge} and c_{Se} respectively.

phase, comprising mobile Cu^+ ions in a bcc lattice of Br^- ions (Boyce and Huberman 1979), to give a liquid with an electrical conductivity of 2.5 Ω^{-1} cm^{-1} at 498 °C (Janz *et al* 1968).

The $S_{\alpha\beta}(Q)$ for the AX melts measured by neutron diffraction are compared in figure 5. All of these liquids were studied using the instrument D4B set-up in the same configuration and the $S_{\alpha\beta}(Q)$ therefore have the same Q-space range and resolution function. It is found that $S_{AA}(Q)$ and $S_{AX}(Q)$ become increasingly structured in the order from CuBr to CuSe via GeSe. For example, whereas the A–A partial structure factor for CuBr is broad and featureless, that for CuSe comprises well defined oscillations. The high-Q oscillations in $S_{XX}(Q)$ for CuBr are more highly damped than for GeSe and CuSe. The corresponding $g_{\alpha\beta}(r)$ are compared in figure 6 and the coordination numbers and interatomic separations are summarized in table 2. In liquid GeSe and CuSe there is clear evidence for both A–A and Se–Se homopolar contacts whereas in the solid state the only homopolar contacts are the Se–Se pairs in CuSe. By contrast, there is no evidence for Br–Br contacts in molten CuBr although short Cu–Cu distances are observed in both the liquid and high-temperature solid phases, in keeping with the relatively high mobility of the Cu^+ ions (Pusztai and McGreevy 1998). In summary, while short A–A distances occur in all three liquids, these nearest-neighbour correlations are better resolved for molten GeSe and CuSe where clearly defined short-ranged Se–Se correlations also occur.

5.3. Comparison with the structure of molten $GeSe_2$

In a previous paper the evolution with x of the topology of the structure in molten Ge_xSe_{1-x} was investigated by using neutron diffraction: since $b(^N\mathrm{Ge}) \approx b(^N\mathrm{Se})$ the measured total structure factors give $S_{NN}^{BT}(Q)$ to a good approximation (Salmon and Liu 1994). It was pointed out that the occurrence of a glass forming region with decreasing x is accompanied by the appearance of a so-called first sharp diffraction peak (FSDP) in $S_{NN}^{BT}(Q)$, i.e. with the development of a

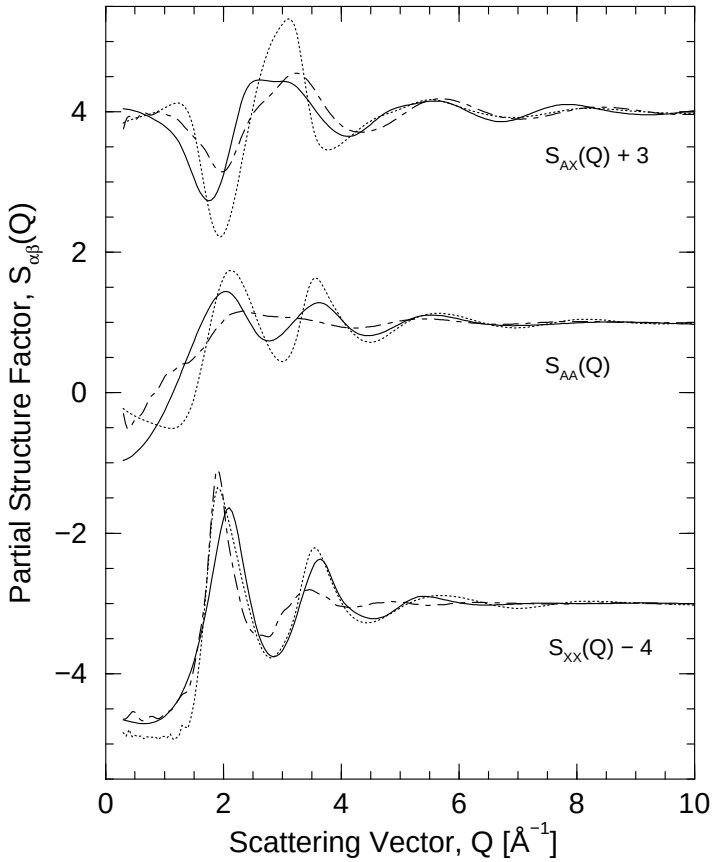

Figure 5. The $S_{\alpha\beta}(Q)$ for liquid GeSe at 727 °C (solid curves), CuSe at 700 °C (dashed curves) and CuBr at 515 °C (dot–dashed curves). The CuBr partial structure factors are taken from Pusztai and McGreevy (1998).

Table 2. Coordination numbers and interatomic separations in the molten AX systems GeSe (present work), CuSe (Barnes and Enderby 1988) and CuBr (see key). The $r_{\alpha\beta}$ denote the mean peak positions in the $g_{\alpha\beta}(r)$.

Liquid	r_{AA} (Å)	$\bar{n}_A^A$	r_{AX} (Å)	$\bar{n}_A^X$	r_{XX} (Å)	$\bar{n}_X^X$
GeSe	2.36(2)	0.8(1)	2.54(2)	3.2(2)	2.34(2)	0.22(3)
	3.81(2)	7.4(3)			3.76(2)	8.6(3)
CuSe	2.43(2)	0.6(3)	2.52(3)	5.6(3)	2.40(2)	0.6(3)
	3.62(2)	10(2)			3.35(2)	10(2)
CuBr[a]	—	—	2.43(2)	3.6(5)	3.89(1)	11.1(1)
CuBr[b]	2.56(2)	1.3(2)	2.39(2)	2.9(2)	4.01(2)	10.2(4)
CuBr[c]	3.0(1)	—	2.37(2)	3.1	3.88(3)	11.4

From the work of [a] Allen and Howe (1992), [b] Pusztai and McGreevy (1998) or [c] Saito *et al* (1997).

second length scale associated with intermediate-range atomic correlations (see e.g. Salmon 1994). The comparison in figure 4 confirms this observation, i.e. at $x = 0.5$ there is a small FSDP at 1.19(2) Å^{-1} in $S_{NN}^{BT}(Q)$ that is not present at $x = 0$ and which develops to be a more significant feature at $x = 1/3$. Moreover, although there is a clearly defined FSDP at

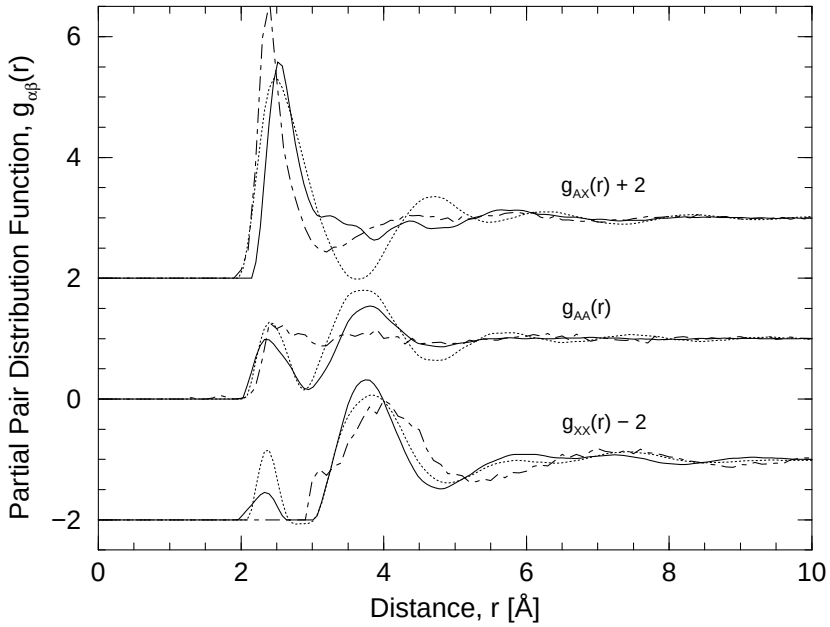

Figure 6. The $g_{\alpha\beta}(r)$ for liquid GeSe at 727 °C (solid curves), CuSe at 700 °C (dashed curves) and CuBr at 515 °C (dot–dashed curves). The CuBr partial pair distribution functions are taken from Pusztai and McGreevy (1998).

0.95(2) Å^{-1} in the measured $S_{CC}^{BT}(Q)$ for molten $GeSe_2$ (Penfold and Salmon 1991, Salmon 1992), no such feature exists for molten GeSe. Overall, the absence in molten GeSe of any strong fluctuations on the scale of the intermediate-range atomic correlations suggests that it may be more amenable to study than $GeSe_2$ by current *ab initio* molecular dynamics methods (see e.g. Massobrio *et al* 1998, 1999).

6. Conclusions

The local ordering in liquid GeSe is significantly different to that of either its high- or low-temperature crystalline forms. Homopolar Ge–Ge and Se–Se bonds are prominent features in the molten state and there are qualitative similarities with the structure of the molten semiconductor CuSe. By comparison, although short A–A distances occur in CuBr, the distribution of these distances is broader and homopolar X–X correlations are not present. The FSDP in $S_{NN}^{BT}(Q)$ for molten GeSe is small relative to that for $GeSe_2$ and there is no FSDP in the other Bhatia–Thornton partial structure factors, i.e. the intermediate-range atomic ordering is weaker than in the glass-forming network melt.

Acknowledgments

We would like to thank Pierre Palleau for valuable help with the experiment, and Drs Adrian Barnes and Robert McGreevy for sending us the data sets for CuSe and CuBr. IP thanks the University of East Anglia for financial support.

References

Allen D A and Howe R A 1992 *J. Phys.: Condens. Matter* **4** 6029
Azoulay R, Thibierge H and Brenac A 1975 *J. Non-Cryst. Solids* **18** 33
Barnes A C and Enderby J E 1988 *Phil. Mag.* B **58** 497
Barnes A C, Lague S B, Salmon P S and Fischer H E 1997 *J. Phys.: Condens. Matter* **9** 6159
Berry L G 1954 *Am. Mineral.* **39** 504
Bertagnolli H, Chieux P and Zeidler M D 1976 *Mol. Phys.* **32** 759
Bhatia A B and Thornton D E 1970 *Phys. Rev.* B **2** 3004
Boyce J B and Huberman B A 1979 *Phys. Rep.* **51** 189
Cobb M and Drabold D A 1997 *Phys. Rev.* B **56** 3054
Cusack N E 1987 *The Physics of Structurally Disordered Matter* (Bristol: Hilger)
Dalba G, Fornasini P, Grazioli M and Rocca F 1995 *Phys. Rev.* B **52** 11 034
Dutta S N and Jeffrey G A 1965 *Inorg. Chem.* **4** 1363
Edwards F G, Enderby J E, Howe R A and Page D I 1975 *J. Phys. C: Solid State Phys.* **8** 3483
Etherington G, Wright A C, Wenzel J T, Dore J C, Clarke J H and Sinclair R N 1982 *J. Non-Cryst. Solids* **48** 265
Glazov V M, Kurbatov V A and Faradzhov A I 1987 *Sov. Phys.–Semicond.* **21** 295
Haye M J, Massobrio C, Pasquarello A, De Vita A, De Leeuw S W and Car R 1998 *Phys. Rev.* B **58** 14 661
Hohl D and Jones R O 1991 *Phys. Rev.* B **43** 3856
Hulliger F 1976 *Physics and Chemistry of Materials with Layered Structures* vol 5, ed F Lévy (Dordrecht: Reidel)
Ipser H, Gambino M and Schuster W 1982 *Monat. Chem.* **113** 389
Jal J F, Mathieu C, Chieux P and Dupuy J 1990 *Phil. Mag.* B **62** 351
Janz G J, Dampier F W, Lakshminarayanan G R, Lorenz P K and Tomkins R P T 1968 *Natl Bur. Stand. Ref. Data Ser.* **15** 1
Kannewurf C R, Kelly A and Cashman R J 1960 *Acta Crystallogr.* **13** 449
Massobrio C, Pasquarello A and Car R 1998 *Phys. Rev. Lett.* **80** 2342
——1999 *J. Am. Chem. Soc.* **121** 2943
Okada T, Satoh T, Matsumura M and Ohno S 1996 *J. Phys. Soc. Japan* **65** 230
Okazaki A 1958 *J. Phys. Soc. Japan* **13** 1151
Penfold I T and Salmon P S 1990 *J. Phys.: Condens. Matter* **2** SA233
——1991 *Phys. Rev. Lett.* **67** 97
——1992 *Phys. Rev. Lett.* **68** 253
Petri I, Salmon P S and Fischer H E 1999 *J. Non-Cryst. Solids* at press
Pusztai L and McGreevy R L 1998 *J. Phys.: Condens. Matter* **10** 525
Ruska J and Thurn H 1976 *J. Non-Cryst. Solids* **22** 277
Saito M, Park C, Omote K, Sugiyama K and Waseda Y 1997 *J. Phys. Soc. Japan* **66** 633
Salmon P S 1988 *J. Phys. F: Met. Phys.* **18** 2345
——1992 *Proc. R. Soc.* A **437** 591
——1994 *Proc. R. Soc.* A **445** 351
Salmon P S and Benmore C J 1992 *Recent Developments in the Physics of Fluids* ed W S Howells and A K Soper (Bristol: Hilger) p F225
Salmon P S and Liu J 1994 *J. Phys.: Condens. Matter* **6** 1449
Salmon P S, Xin S and Fischer H E 1998 *Phys. Rev.* B **58** 6115
Sears V F 1992 *Neutron News* **3** 26
Tronc P, Bensoussan M, Brenac A and Sebenne C 1973 *Phys. Rev.* B **8** 5947
Tsuchiya Y 1990 *J. Non-Cryst. Solids* **122** 205
Vashishta P, Kalia R K, Antonio G A and Ebbsjö I 1989a *Phys. Rev. Lett.* **62** 1651
Vashishta P, Kalia R K and Ebbsjö I 1989b *Phys. Rev.* B **39** 6034
Wiedemeier H and Siemers P A 1975 *Z. Anorg. (Allg.) Chem.* **411** 90